Cooling of a trapped ion in the strong-sideband regime

C. A. Blockley and D. F. Walls
Department of Physics, University of Auckland, Private Bag 92019, Auckland, New Zealand
(Received 24 September 1992)

A single two-level atom, with quantized center-of-mass motion, is constrained to move in a one-dimensional harmonic potential while interacting with a single-mode classical traveling-wave light field. When the classical light field is tuned to the atom's lower vibrational sideband, cooling can occur. The strong-sideband and Lamb-Dicke perturbation regimes for the system are defined. The steady-state and time-evolution behaviors in the strong-sideband regime are discussed and, in particular, it is shown that the steady-state average trap number saturates when spontaneous emission is weak and that the steady-state average trap number depends more strongly on the trap frequency in the saturated regime than previously predicted. Finally, the possibility of observing quantum jumps between trap levels is discussed.

PACS number(s): 32.80.Pj, 42.50.Vk

I. INTRODUCTION

The cooling and trapping of atoms and ions is currently attracting considerable experimental and theoretical interest. The goal of cooling and trapping is the ability to control the state of motion of atoms or ions by utilizing their mechanical interaction with light. A single trapped and cooled ion provides an ideal system for carrying out investigations in quantum optics, as well as having promising applications in precision spectroscopy and time and frequency standards.

In this paper we are concerned with laser cooling of a single two-level ion in a harmonic potential. In the case of a Paul trap, the harmonic potential is provided by an oscillating electric quadrupole field. The motion of a single ion in such a trap can be thought of as a secular harmonic motion in the trapping potential and a micromotion at the frequency of the oscillating electromagnetic field. When the ion's absorption sidebands are well resolved (known as the resolved-sideband limit: $\nu \gg \Gamma$, where ν is the trap frequency and Γ is the spontaneous emission rate) the traveling wave can be used to excite the ion's first lower vibrational sideband, and in so doing energy is absorbed from the vibrational motion of the ion and dissipated via spontaneous emission. In this way the ion is optically pumped into its lowest vibrational state and very low temperatures can be obtained.

This type of cooling is known as sideband cooling and was first reported by Neuhauser *et al.* [1], who also calculate the final cooling energy. Further theoretical investigations are carried out in [2], where the irradiating laser is assumed to be at low intensity. In [3] the effect of finite laser bandwidth and the energy of the radiofrequency micromotion are included. Saturation effects are included in [4–6], the method subsequently being refined to take into account anomalous coherence effects [7,8]. A summary of results can be found in [9].

The above calculations were carried out in a regime where it is assumed that the dominant coherent processes do not change the trap state. Such a regime can be obtained by going to the Lamb-Dicke limit, where the ion is localized to dimensions much smaller than the wavelength of the driving field. The major advantage of such a regime is that a perturbation expansion can be carried out which leads to analytic solutions for the steady-state energy and the cooling rates [6–8]. This regime will be referred to as the Lamb-Dicke perturbation (LDP) regime.

But coherent processes which do not change the trap state need not dominate. If the driving field is tuned to the first lower vibrational sideband and if the trap levels are well spaced, $\nu \gg \Omega$ (where Ω is the Rabi frequency), processes involving off-resonant transitions go as $(\Omega/\nu)^2$. There are, therefore, two competing effects. In the Lamb-Dicke limit processes involving the sidebands are small, while large ν tends to make the nonresonant processes small. In the LDP regime the former effect is dominant, and if the latter effect is dominant we call the regime the strong-sideband (SSB) regime.

In this paper a master equation for laser cooling in a trap, derived by Stenholm and co-workers [6,8], will be used to consider the system in the SSB regime. In Sec. II the model is introduced and the equations of motion for the density operator are obtained. The SSB regime is defined in Sec. III and a perturbation expansion is developed which reduces the number of equations which need to be solved. In Sec. IV simulations of the steady-state average trap number $\langle n \rangle_c$ are carried out for various regions of the parameter space. It is seen that $\langle n \rangle_c$ saturates when coherent processes dominate over incoherent. In the saturation regime $\langle n \rangle_c$ depends inversely on the fourth power of the trap frequency as opposed to the usual second power result [9]. In Sec. V simulations of the time dependence of the average trap number $\langle n \rangle$ are carried out. It is noted, in particular, that transient coherent effects can increase the cooling time, as well as leading to quantum collapses and revivals in $\langle n \rangle$.

One of the applications of trapped ions has been the ability to observe, for extended periods, the fluorescence from a single ion. This has made possible the study of quantum jumps [10–14]. In the experiments to date

quantum jumps have been observed between internal energy states of an atom, and in Sec. VI we ask whether the simple model of laser cooling under discussion would enable the observation of quantum jumps between vibrational states of an ion in a trap. To this end a stochastic simulation of an ion in a trap is carried out. Stochastic simulations of cooling have already been carried out in [15], where they are used to obtain ensemble behavior. Our simulations are based on the approach in [16,17].

II. THE MODEL AND THE EQUATIONS OF MOTION

We consider an ideal two-level ion of mass m constrained to move in a three-dimensional harmonic potential. The problem becomes one dimensional if one of the principal trap axes is taken to coincide with the axis along which the driving field propagates, taken to be the z axis. Instead of the triplet of quantum numbers (n_1,n_2,n_3) labeling the vibrational states of the trap, one quantum number now suffices. The other two are traced out by summing over the corresponding degrees of freedom. In one dimension, therefore, the oscillator states for the ion have the energies

$$E_n=\hbar\nu(n+\tfrac{1}{2}) , \tag{1}$$

where the n are the occupation numbers for the trap states and ν is the characteristic trap frequency for the mode along the principal trap axis. The energy levels corresponding to the internal electronic degrees of freedom and the external vibrational degrees of freedom are shown in Fig. 1. Number states $|n\rangle$ can be used as eigenstates for the vibrational states, while creation and annihilation operators, $a^\dagger$ and a, ladder between the states. The operators are related to the ion's position and momentum operators according to

$$z=\sqrt{\hbar/2\nu m}\,(a+a^\dagger),\quad p=i\sqrt{\hbar\nu m/2}(a^\dagger-a) . \tag{2}$$

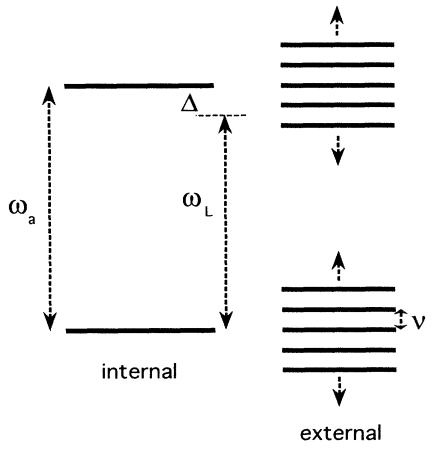

FIG. 1. The energy-level structure for the internal and external degrees of freedom for an ion in a trap of characteristic frequency ν interacting with a classical traveling-wave light field of frequency ω_L. The ion has an atomic transition frequency ω_a and is detuned by an amount Δ from the driving field.

The internal states of the ion are labeled $|e\rangle$ and $|g\rangle$ for the excited and ground states, respectively, and the energy difference is $\hbar\omega_{ge}$. The operators σ_z, σ^+, and σ^- act on this internal space in the usual way. The ion's internal and external degrees of freedom are coupled together by a traveling light field given by

$$\mathbf{E}(\mathbf{x})=E\mathbf{e}\cos(\omega_L t-kz) , \tag{3}$$

where $\mathbf{e}$ is the polarization vector and k is the wave vector. In the dipole approximation the transition matrix element is

$$\langle e,n|\mathbf{D}\cdot\mathbf{E}|g,n'\rangle=\tfrac{1}{2}\hbar\Omega[\,e^{i\omega_L t}u^*_{n,n'}(k)+e^{-i\omega_L t}u_{n,n'}(k)] , \tag{4}$$

where $u_{n,n'}(k)=\langle n|e^{ikx}|n'\rangle$ and Ω is the Rabi frequency $\Omega=(E/\hbar)\langle e|\mathbf{e}\cdot\mathbf{D}|g\rangle$.

The part of the Hamiltonian which gives the free energy and the coherent interaction between the traveling wave and the ion is

$$H_1=\hbar\nu(a^\dagger a+\tfrac{1}{2})+\tfrac{1}{2}\hbar\omega_{ge}\sigma_z +\tfrac{1}{2}\hbar\Omega(F\sigma^+e^{-i\omega_L t}+F^*\sigma^-e^{i\omega_L t}) , \tag{5}$$

where $F\equiv e^{ikz}=e^{i\epsilon(a^\dagger+a)}$.

The Lamb-Dicke parameter ϵ is given by $\epsilon=(E_r/E_\nu)^{1/2}$, where $E_r=\hbar^2k^2/2m$ is the classical recoil energy of the ion and $E_\nu=\hbar\nu$ is the energy of a trap quantum. In the classical limit, with trap states very close together, ϵ is large, and the absorption or emission of a photon will always cause some change in the vibrational state of the atom. In the nonclassical or Lamb-Dicke limit of small ϵ, the trap states are well spaced, and many photons may need to be absorbed or emitted before the atom changes vibrational state.

Spontaneous emission can be included in this system by coupling to the vacuum field given by the operators $b^\dagger_{\mathbf{k}}$ and $b_{\mathbf{k}}$, which create and annihilate photons of energy $\hbar\omega_{\mathbf{k}}$ in the mode $|\mathbf{k}\rangle$. The Hamiltonian describing the process is

$$H_2=\hbar\sum_{\mathbf{k}'}{}'\,\omega_{\mathbf{k}'}b^\dagger_{\mathbf{k}'}b_{\mathbf{k}'}-\hbar\sum_{\mathbf{k}'}g(\mathbf{k}')(F\sigma^+b_{\mathbf{k}'}+F^*\sigma^-b^\dagger_{\mathbf{k}'}) , \tag{6}$$

where the coupling constant is

$$g(\mathbf{k})=\frac{1}{\hbar}\langle e|\mathbf{e}\cdot\mathbf{D}|g\rangle\left[\frac{\hbar\omega_{\mathbf{k}}}{2\epsilon_0 V}\right]^{1/2} . \tag{7}$$

The prime on the summation is a reminder that the strong mode when $\mathbf{k}'=\mathbf{k}$ is excluded.

The equation of motion for the density operator is

$$\dot\rho=-\frac{i}{\hbar}[H_1,\rho]+\rho_\tau , \tag{8}$$

where ρ_τ is the relaxation term due to the spontaneous emission model by H_2, and can be derived in a standard way by regarding the vacuum as a heat bath [18]. The density operator matrix elements can be defined as

$$\rho_{\alpha\beta}(n,n')=\langle\alpha,n|\rho|\beta,n'\rangle\ , \tag{9}$$

where $\alpha,\beta\in\{g,e\}$. We also remove the fast oscillation at the frequency of the driving field

$$\tilde{\rho}_{eg}(n,n')=e^{i\omega_L t}\rho_{eg}(n,n')\ . \tag{10}$$

The equations of motion become

$$\begin{aligned}
\dot{\rho}_{ee}(n,n')&=-[i\nu'(n-n')+\Gamma']\rho_{ee}(n,n')\\
&\quad+\frac{i}{2}\sum_m[\tilde{\rho}_{eg}(n,m)u^*_{m,n'}-u_{n,m}\tilde{\rho}_{ge}(m,n')]\ ,\\
\dot{\rho}_{gg}(n,n')&=-i\nu'(n-n')\rho_{gg}(n,n')\\
&\quad+\frac{i}{2}\sum_m[\tilde{\rho}_{ge}(n,m)u_{m,n'}-u^*_{n,m}\tilde{\rho}_{eg}(m,n')]\\
&\quad+\frac{\Gamma'}{4\pi}\sum_{m,m'}\int d^2\Omega\,\Theta(\hat{\mathbf{k}})u_{n,m}(k_z)\\
&\qquad\times\rho_{ee}(m,m')u^*_{m',n'}(k_z)\ ,\\
\dot{\tilde{\rho}}_{eg}(n,n')&=-[i\nu'(n-n')+i\Delta'+\Gamma'/2]\tilde{\rho}_{eg}(n,n')\\
&\quad+\frac{i}{2}\sum_m[\rho_{ee}(n,m)u_{m,n'}-u_{n,m}\rho_{gg}(m,n')]\ ,
\end{aligned} \tag{11}$$

and $\tilde{\rho}_{ge}(n,n')=[\tilde{\rho}_{eg}(n',n)]^*$. The derivatives are with respect to the scaled time parameter $\tau=\Omega t$. The parameters Γ' and ν' are the spontaneous emission rate and the trap frequency scaled by the Rabi frequency. Δ' is the detuning given by

$$\Delta'=(\omega_{ge}-\omega_L)/\Omega\ . \tag{12}$$

The integration $\int d^2\Omega$ is over all directions of the outgoing radiation, weighted by the angular distribution function $\Theta(\hat{\mathbf{k}})$. The wave vector of the spontaneous photon is described by a unit direction vector $\hat{\mathbf{k}}$ and a magnitude $|\mathbf{k}|$ and has a component k_z in the z direction. In what follows the angular distribution of spontaneously emitted photons will be assumed to be isotropic: $\Theta(\hat{\mathbf{k}})=1$. The integration can be carried out by changing the integration variables to the spherical polar coordinates θ and ϕ:

$$\int d^2k=\int d\theta d\phi\sin\theta\ . \tag{13}$$

The matrix elements under the integral have a dependence on θ,

$$u_{n,m}(k_z)=\langle n|e^{ik_z z}|m\rangle=\langle n|e^{i|\mathbf{k}|z\cos\theta}|m\rangle \tag{14}$$

and when the integration is carried out the recoil term becomes

$$\begin{aligned}
Q(n,n')&=\frac{\Gamma}{2|\mathbf{k}|}\sum_{m,m'}\int_{-|\mathbf{k}|}^{|\mathbf{k}|}dk'u_{n,m}(k')\rho_{ee}(m,m')u^*_{m',n'}(k')\\
&\equiv\Gamma\sum_{m,m'}\lambda^{(n)(n)'}_{mm'}\ .
\end{aligned} \tag{15}$$

The $u_{n,n'}$ are matrix elements of F between the number states, and give the strength of the coupling between different vibrational states. They can be evaluated by writing F as a series in the operators a and $a^\dagger$, and acting with these left and right on the number states. The result for $n\geq n'$ is

$$u_{n,n'}=e^{-\epsilon^2/2}(i\epsilon)^{n'-n}\left[\frac{n!}{n'!}\right]^{1/2}L_n^{n'-n}(\epsilon^2)\ , \tag{16}$$

where $L_n^{n'-n}$ is an associated Laguerre polynomial. $u_{n,n'}$ is symmetric on interchange of its indices. In the Lamb-Dicke limit $u_{n,n'}$ can be expanded in powers of ϵ giving

$$\begin{aligned}
u_{m,m}&=1\ ,\\
u_{m,m+1}&=i\epsilon\sqrt{m+1}
\end{aligned} \tag{17}$$

as the only nonzero terms to first order in ϵ.

III. THE STRONG-SIDEBAND REGIME

The equations of motion for the density operator matrix elements form an infinite set of coupled linear differential equations, and if they are to be solved analytically an approximation must be made. One of the most popular approximations [1,2,6–8] is to assume that the dominant coherent process is a Rabi cycling between states with the same trap quantum number n (LDP regime). In the Lamb-Dicke regime coherent processes which change the trap quantum number by one will be proportional to ϵ (or higher powers of ϵ), and in the limit that $\epsilon\ll 1$, these processes will be weak compared to the Rabi cycling between states with the same trap quantum number. This limit can be quantified by introducing an absorption line shape for the ion

$$P(x)=\frac{\Gamma'/4}{x^2+\Gamma'^2/4}\ . \tag{18}$$

When the traveling light field is detuned by an amount Δ' from the atomic resonance and the ion is in the state $|g,n\rangle$, the rates for transitions to the states $|e,n\rangle$, $|e,n-1\rangle$, and $|e,n+1\rangle$ are $|u_{n,n}|^2P(\Delta')$, $|u_{n,n-1}|^2P(\Delta'-\nu')$, and $|u_{n,n+1}|^2P(\Delta'+\nu')$, respectively.

The system is in the LDP regime, therefore, when

$$\begin{aligned}
|u_{n,n}|^2P(\Delta')&\gg|u_{n,n-1}|^2P(\Delta'-\nu')\ ,\\
|u_{n,n}|^2P(\Delta')&\gg|u_{n,n+1}|^2P(\Delta'+\nu')\ .
\end{aligned} \tag{19}$$

When the driving field is tuned to the ion's first lower sideband, $\Delta'=\nu'$, and the system is in the resolved-sideband regime, the first condition becomes

$$\left[\frac{\Gamma'}{2\nu'}\right]^2\gg\epsilon^2\ , \tag{20}$$

while the second condition restates the Lamb-Dicke limit.

We are interested in the behavior of the system in the SSB regime, where the trap levels are well spaced, $\nu'\gg 1$, such that transitions between the states $|g,n\rangle$ and $|e,n-1\rangle$ will be strong compared with other transitions. In this case the relationship between the strengths of the various transitions becomes

$$\begin{aligned}
|u_{n,n}|^2P(\Delta')&\ll|u_{n,n-1}|^2P(\Delta'-\nu')\ ,\\
|u_{n,n+1}|^2P(\Delta'+\nu')&\ll|u_{n,n-1}|^2P(\Delta'-\nu')\ .
\end{aligned} \tag{21}$$

When the driving field is tuned to the ion's first lower sideband, $\Delta'=\nu'$, and the system is in the resolved-sideband regime, the condition for the SSB regime becomes

$$\left[\frac{\Gamma'}{2\nu'}\right]^2 \ll \epsilon^2 . \tag{22}$$

The LDP regime corresponds to an absorption spectrum (Fig. 2) where the central line at the atomic frequency is the strongest, and the sidebands are weak. The SSB regime corresponds to an absorption spectrum where the first lower sideband is the strongest, and other lines are weak.

The behavior of a trapped ion has already been studied in the SSB regime [19], and it was shown that quantum collapses and revivals occur. One of the most recent experiments on sideband cooling, by Wineland and coworkers [20], is also carried out in this regime. In [20] the narrow $^2S_{1/2}$-$^2D_{5/2}$ electric-quadrupole transition in $^{198}Hg^+$ is used to cool the ion. The trap frequency is $\nu=2.96$ MHz, the decay rate is $\Gamma=11$ Hz [21], and the wavelength of the transition is $\lambda=281.5$ nm. These parameters give $\epsilon\sim 0.07$ and $(\Gamma'/2\nu'\epsilon)^2\sim 1.7\times 10^{-10}$.

Perturbation expansion in the resolved-sideband limit

In the resolved-sideband limit, a perturbation expansion can be developed in the small parameter Γ'/ν'. We also assume the system to be in the strong-trap limit, $\nu'\gg 1$, so that a simultaneous expansion can be carried out in $1/\nu'$. This perturbation expansion will allow a division into quickly and slowly varying density operator matrix elements, the former of which can be adiabatically eliminated.

In this perturbation expansion the populations of the upper and lower electronic states and the coherences between the states $|e,n\rangle$ and $|g,n+1\rangle$ are slowly varying and can be written as

$$\begin{aligned}
\dot{\rho}_{ee}(n,n) &= -\Gamma'\rho_{ee}(n,n)+\frac{i}{2}[\tilde{\rho}_{eg}(n,n+1)u^*_{n+1,n}-u_{n,n+1}\tilde{\rho}_{ge}(n+1,n)] \\
&\quad +\frac{i}{2}\sum_{m\ (\neq n+1)}[\tilde{\rho}_{eg}(n,m)u^*_{m,n}-u_{n,m}\tilde{\rho}_{ge}(m,n)] , \\
\dot{\tilde{\rho}}_{gg}(n,n) &= \frac{i}{2}[\tilde{\rho}_{ge}(n,n-1)u_{n-1,n}-u^*_{n,n-1}\tilde{\rho}_{eg}(n-1,n)] \\
&\quad +\frac{i}{2}\sum_{m\ (\neq n-1)}[\tilde{\rho}_{ge}(n,m)u_{m,n}-u^*_{n,m}\tilde{\rho}_{eg}(m,n)]+Q(n,n) , \\
\dot{\tilde{\rho}}_{eg}(n,n+1) &= -\tfrac{1}{2}\Gamma'\tilde{\rho}_{eg}(n,n+1)+\frac{i}{2}[\rho_{ee}(n,n)u_{n,n+1}-u_{n,n+1}\rho_{gg}(n+1,n+1)] \\
&\quad +\frac{i}{2}\sum_{m\ (\neq n)}\rho_{ee}(n,m)u_{m,n+1}-\frac{i}{2}\sum_{m\ (\neq n+1)}u_{n,m}\rho_{gg}(m,n+1) ,
\end{aligned} \tag{23}$$

and $\tilde{\rho}_{ge}(n,n')=[\tilde{\rho}_{eg}(n',n)]^*$. The mean values of the quickly varying variables,

$$\begin{aligned}
\rho_{ee}(n,n') &= \frac{i/2}{i\nu'(n-n')+\Gamma'} \\
&\quad \times\sum_m[\tilde{\rho}_{eg}(n,m)u^*_{m,n'}-u_{n,m}\tilde{\rho}_{ge}(m,n')] \\
&\quad (n\neq n') , \\
\rho_{gg}(n,n') &= \frac{i/2}{i\nu'(n-n')}\sum_m[\tilde{\rho}_{ge}(n,m)u_{m,n'} \\
&\quad -u^*_{n,m}\tilde{\rho}_{eg}(m,n')] \\
&\quad +\frac{Q(n,n')}{i\nu'(n-n')} \quad (n\neq n') , \\
\tilde{\rho}_{eg}(n,n') &= \frac{i/2}{i\nu'(n-n'+1)+\Gamma'/2} \\
&\quad \times\sum_m[\rho_{ee}(n,m)u_{m,n'}-u_{n,m}\rho_{gg}(m,n')] \\
&\quad (n\neq n'+1) , \\
\tilde{\rho}_{ge}(n,n') &= \frac{i/2}{i\nu'(n-n'-1)+\Gamma'/2} \\
&\quad \times\sum_m[\rho_{gg}(n,m)u^*_{m,n'}-u^*_{n,m}\rho_{ee}(m,n')] \\
&\quad (n\neq n'-1) ,
\end{aligned} \tag{24}$$

can be expanded recursively to the required order in $1/\nu'$ and Γ'/ν' and substituted back into Eq. (23). In the Lamb-Dicke limit, $\epsilon<1$, a simultaneous expansion in the small parameter ϵ/ν' can also be carried out.

It should also be noted that in solving these equations for the density matrix the equations must be truncated for some value of the trap quantum number n. This should not be a problem as initial coherent or thermal states for the trap tend to zero for large n and cooling should give probability distributions which are peaked at $n=0$. If the equations are truncated at $n=N$ there will be $4(N+1)$ equations to solve after adiabatic elimination rather than $4(N+1)^2$ for the full density operator.

IV. THE STEADY STATE

A. The LDP regime

The average trap quantum number is given by

$$\begin{aligned}
\langle n\rangle &= \mathrm{Tr}(a^\dagger a\rho) \\
&= \sum_n n[\rho_{gg}(n,n)+\rho_{ee}(n,n)] ,
\end{aligned} \tag{25}$$

and is calculated in the LDP regime for the steady state in [6] from rate equation considerations and in [7,8] in-

cluding coherences. For isotropic spontaneous emission and for no phase relaxation the steady-state average trap number is given in the resolved-sideband limit, $\Gamma' \ll \nu'$, by

$$\langle n \rangle_c = \frac{7}{48}\left[\frac{\Gamma'}{\nu'}\right]^2 . \tag{26}$$

The initial analysis of [6], while not correct in detail, does give some insight into the physical processes at work in the cooling. The argument leading to the final temperature will be sketched here and used to give some understanding of the behavior of the steady-state average trap number in the SSB regime.

The derivation of the steady state in [6] begins with the master equation [Eq. (11)], from which rate equations for the populations are obtained:

$$\begin{aligned}
\dot{\rho}_{ee}(n,n) &= -\Gamma'\rho_{ee}(n,n) + \frac{\epsilon^2(n+1)}{\Gamma'}[\rho_{gg}(n+1,n+1)-\rho_{ee}(n,n)] + \frac{\Gamma'/4}{\nu'^2+\Gamma'^2/4}[\rho_{gg}(n,n)-\rho_{ee}(n,n)] \\
&\quad + \frac{\epsilon^2 n\Gamma'/4}{4\nu'^2+\Gamma'^2/4}[\rho_{gg}(n-1,n-1)-\rho_{ee}(n,n)] , \\
\dot{\rho}_{gg}(n,n) &= \frac{\epsilon^2 n}{\Gamma'}[\rho_{ee}(n-1,n-1)-\rho_{gg}(n,n)] + \frac{\Gamma'/4}{\nu'^2+\Gamma'^2/4}[\rho_{ee}(n,n)-\rho_{gg}(n,n)] \\
&\quad + \frac{\epsilon^2(n+1)\Gamma'/4}{4\nu'^2+\Gamma'^2/4}[\rho_{ee}(n,n)-\rho_{gg}(n,n)] + \Gamma'[1-\tfrac{1}{3}\epsilon^2(2n+1)]\rho_{ee}(n,n) \\
&\quad + \tfrac{1}{3}\Gamma'\epsilon^2[(n+1)\rho_{ee}(n+1,n+1)+n\rho_{ee}(n-1,n-1)] .
\end{aligned} \tag{27}$$

The important processes which change the trap number are shown in Fig. 3. In Fig. 3(a) Rabi cycling between $|g,n\rangle$ and $|e,n\rangle$ is followed by spontaneous emission to $|g,n+1\rangle$. In Fig. 3(b) Rabi cycling between $|g,n+1\rangle$ and $|e,n+1\rangle$ is followed by spontaneous emission to $|g,n\rangle$. In Fig. 3(c) Rabi cycling between $|g,n+1\rangle$ and $|e,n\rangle$ is followed by spontaneous emission to $|g,n\rangle$. In Fig. 3(d) Rabi cycling between $|g,n\rangle$ and $|e,n+1\rangle$ is followed by spontaneous emission to $|g,n+1\rangle$. The rates at which these processes proceed are given by

$$R_a = \tfrac{1}{3}\Gamma'\epsilon^2(n+1)P(\Delta') , \tag{28}$$

$$R_b = R_a , \tag{29}$$

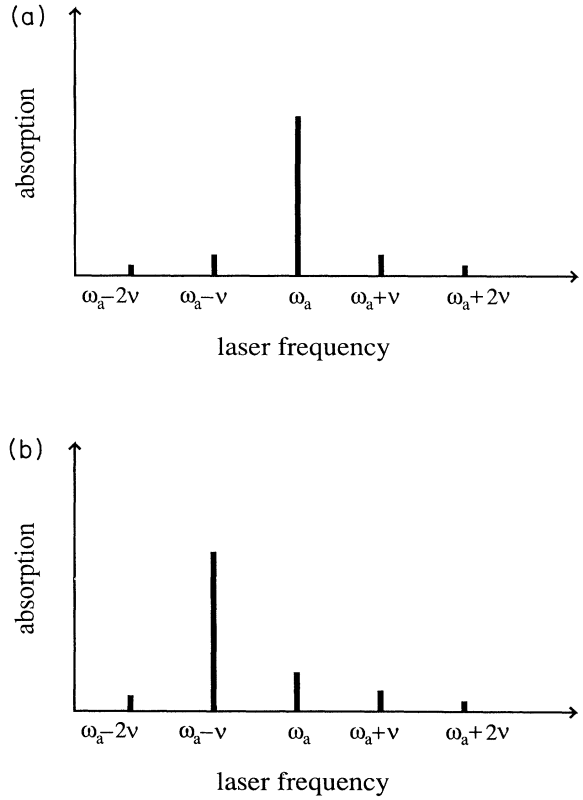

FIG. 2. The absorption spectrum (in schematic form) for a trapped ion as a function of the frequency of the driving field, in the (a) LDP and (b) SSB regime.

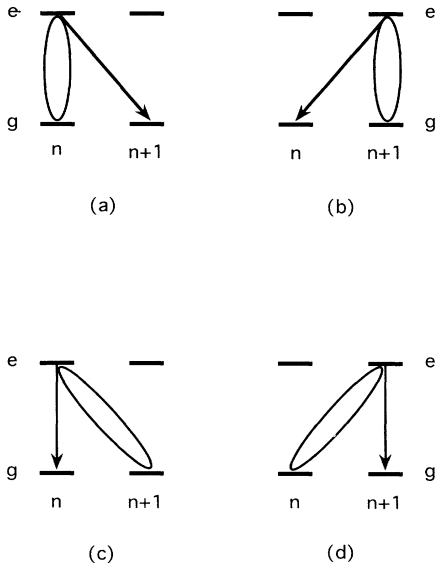

FIG. 3. The dominant processes considered in the determination of the steady-state average quantum number in the LDP regime [6].

$$R_c=\Gamma'\epsilon^2(n+1)P(\Delta'-\nu') , \tag{30}$$

$$R_d=\Gamma'\epsilon^2(n+1)P(\Delta'+\nu') . \tag{31}$$

In the LDP regime a rate equation for the total probability for the ion to be in the nth trap state, $f(n)$, can be written. If the only significant contributions come from the processes shown in Fig. 3 then detailed balance of the transition rates between the states n and $n+1$ gives

$$A_+f(n)=A_-f(n+1) , \tag{32}$$

where $A_+=R_a+R_d$ and $A_-=R_b+R_c$. This gives rise to a Planckian-type distribution for $f(n)$ and if $A_- \gg A_+$ then the average trap number is given by

$$\langle n \rangle_c=\frac{A_+}{A_-} \tag{33}$$

to first order in A_+/A_-. When the rates are evaluated for optimum detuning, that is, $\Delta'=\nu'$, the standard result of Eq. (26) is obtained.

B. The SSB regime

There would seem to be no simple analytic solution to the master equation [Eq. (11)] in the SSB regime, as all the density matrix elements are coupled together by the coherent driving between $|g,n+1\rangle$ and $|e,n\rangle$ followed by spontaneous emission. It might be hoped that the perturbation expansion [Eq. (23)] introduced in Sec. III A could be used but that would require that terms up to at least order ϵ^2/ν'^2 be included, as it was seen in the preceding section that lowest-order heating terms are of order ϵ^2/ν'^2. But this gives no simple rate equation as in [6–8].

The steady state is found, rather, by numerical evaluation of the truncated system, which is carried out by writing Eq. (11) in matrix form and calculating the orthonormal basis vector for the null space of the coefficient matrix. The spontaneous emission recoil term [Eq. (15)] is not included in full, but is expanded to second order in the Lamb-Dicke parameter ϵ.

It should be noted [7] that this truncation leads to nonconservation of probability in the system, as there is some probability that an excited-state ion will decay into a ground state with $n > N$. In order to ensure the conservation of probability the spontaneous emission rate needs to be modified by replacing

$$\Gamma'\rho_{ee}(n,n')\rightarrow\Gamma'_{nn'}\rho_{ee}(n,n')=\tfrac{1}{2}(\Gamma'_n+\Gamma'_{n'})\rho_{ee}(n,n') , \tag{34}$$

where

$$\Gamma'_n=\frac{\Gamma'}{2|\mathbf{k}|}\sum_{m=0}^{N}\int_{-|\mathbf{k}|}^{|\mathbf{k}|}dk'u_{n,m}(k')u^*_{m,n}(k') . \tag{35}$$

The behavior of $\langle n \rangle_c$ as a function of the detuning is shown in Fig. 4. The global minimum occurs when the driving field is on resonance with the first lower sideband, $\Delta'=\nu'$, as expected. There are also local minima corresponding to resonances with the second and third lower sidebands. The temperature in these cases is higher because there is no pumping of the $n=1$ (or $n=2$ in the case of $\Delta'=3\nu'$) states to $n=0$.

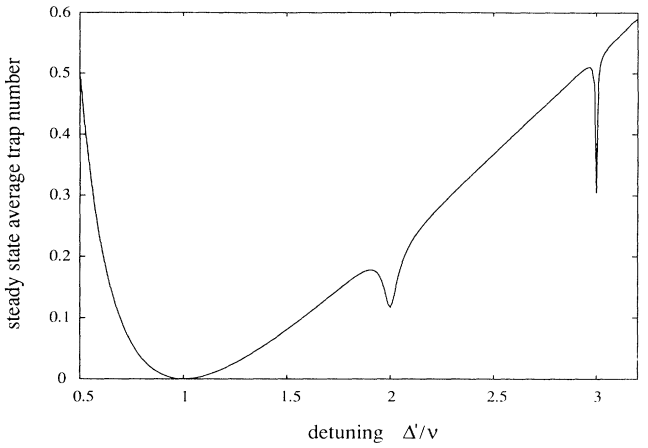

FIG. 4. The steady-state average trap number as a function of the detuning scaled by the trap frequency. Parameters are $\nu'=1000$, $\Gamma'=0.01$, $\epsilon=0.07$, and $N=10$.

Figure 5 shows the behavior of $\langle n \rangle_c$ as a function of the scaled spontaneous emission rate for various values of the trap frequency. In the LDP regime the cooling is always enhanced by decreasing the spontaneous emission, whereas in the SSB regime saturation occurs as the spontaneous emission is decreased. At some stage the ion, when excited into the $|e,n\rangle$ state, is more likely to be coherently cycled between $|e,n\rangle$ and $|g,n+1\rangle$ rather than decaying back to $|g,n\rangle$. One of the set of traces in the figure corresponds to solutions of the simplified equations of motion [Eq. (27)]. They show saturation occur-

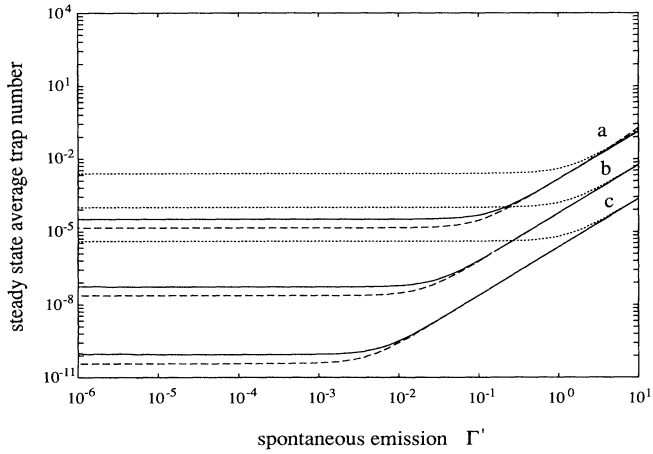

FIG. 5. The steady-state average trap number as a function of the scaled spontaneous emission rate for various values of the scaled trap frequency. The parameters are $N=15$, $\epsilon=0.001$, and $\nu'=10,50,250$, labeled (a)–(c), respectively. The solid line is the solution of the full equations [Eq. (11)], the dotted line is the solution to the rate equations [Eq. (27)], and the dashed line is the analytic result given in Eq. (38).

ring at the same spontaneous emission rate for all three choices of the trap frequency. When the full equations [Eq. (11)] are solved the point at which saturation occurs is dependent on the trap frequency. The result of this is that the steady-state average trap number is more strongly dependent on the trap frequency for small spontaneous emission rates than for large spontaneous emission rates.

A semiqualitative analysis of this effect can be obtained from the expansion procedure outlined in Sec. III A. The highest-order correction to the equation of motion for the coherence $\tilde{\rho}_{eg}(n,n+1)$ in Eq. (23) is frequency dependent:

$$\dot{\tilde{\rho}}_{eg}(n,n+1)=-\tfrac{1}{2}\Gamma'\tilde{\rho}_{eg}(n,n+1)+\frac{i}{2}[\rho_{ee}(n,n)-\rho_{gg}(n+1,n+1)]u_{n,n+1}-\frac{1}{2}\frac{1}{-i\nu'+\Gamma'}\tilde{\rho}_{eg}(n,n+1)+O\left[\frac{\epsilon^2}{\nu}\right] . \tag{36}$$

This additional term is not present in the rate equations [Eq. (27)] and leads to a modification of the transition rate R_c such that

$$A_-|_{\Delta'=\nu'}=\frac{\epsilon^2}{2}\frac{2\nu'^2\Gamma'+\Gamma'(1+\Gamma'^2)}{(1+\Gamma'^2)^2+(\nu'\Gamma')^2}+\frac{\epsilon^2}{3}\frac{\Gamma'/4}{\nu'^2+\Gamma'^2/4} . \tag{37}$$

The steady-state average trap number is now

$$\langle n\rangle_e=\frac{7}{24\nu'^2}\frac{(1+\Gamma'^2)^2+(\nu'\Gamma')^2}{1+\Gamma'^2+2\nu'^2} . \tag{38}$$

For $(\nu'\Gamma')^2\ll 1$ and $\Gamma'^2\ll 1$ the average trap number exhibits saturation. In this regime $\langle n\rangle_c$ goes inversely as the fourth power of the trap frequency

$$\langle n\rangle_c=\frac{7}{48\nu'^4} . \tag{39}$$

The analytical result of Eq. (38) is also shown in Fig. 5. The transition from a $1/\nu'^2$ to a $1/\nu'^4$ dependence for the steady-state average trap number can also be seen clearly in Fig. 6.

This argument should be considered to be only semiquantitative because terms of order ϵ^2/ν'^2 are included in the calculation of $\langle n\rangle_c$ via the transition rate R_d, but are neglected in the expansion leading to Eq. (36). If an attempt were made to consistently include all terms to order ϵ^2/ν'^2 Eq. (36) would no longer allow an easy interpretation in terms of transition rates.

In the LDP regime $\langle n\rangle_c$ does not depend on the Lamb-Dicke parameter ϵ. In the SSB regime $\langle n\rangle_c$ will also not depend on ϵ for sufficiently small values of ϵ. But in both regimes, as ϵ is increased in size towards unity, the terms in the coupling matrix $u_{n,m}$ which are of higher order in ϵ will increasingly come into play. For instance, rather than only the heating process $|g,n\rangle\rightarrow|e,n\rangle\rightarrow|g,n+1\rangle$ (goes as ϵ^2) occurring, there will also be $|g,n\rangle\rightarrow|e,n\rangle\rightarrow|g,n+2\rangle$ (goes as ϵ^4). The growing strength of such terms should lead to a quadratic dependence of $\langle n\rangle_c$ on ϵ. The independence of $\langle n\rangle_c$ on ϵ for small ϵ can be seen in both Figs. 7 and 8.

The saturation behavior can also be seen in Fig. 9. The ϵ-independent behavior can be seen for small Γ'. For small ϵ saturation occurs at essentially the same value of Γ'. As ϵ increases saturation occurs for higher values of Γ'. This is due to the fact that the coherent oscillation

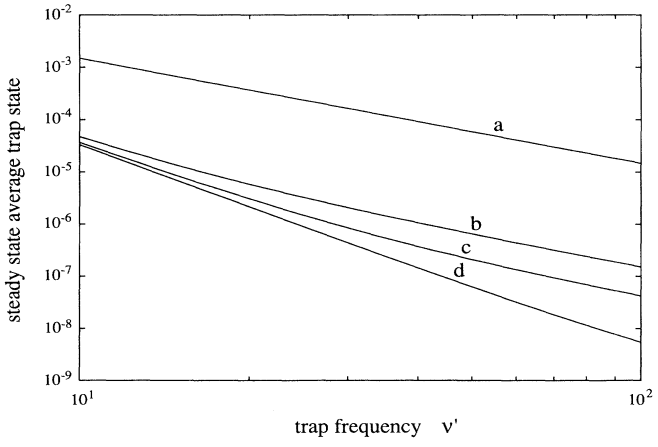

FIG. 6. The steady-state average trap number as a function of the scaled trap frequency for various values of the scaled spontaneous emission $N=5$, $\epsilon=0.01$. The values of the scaled spontaneous emission are $\Gamma'=1,0.1,0.05,0.001$, labeled (a)–(d), respectively.

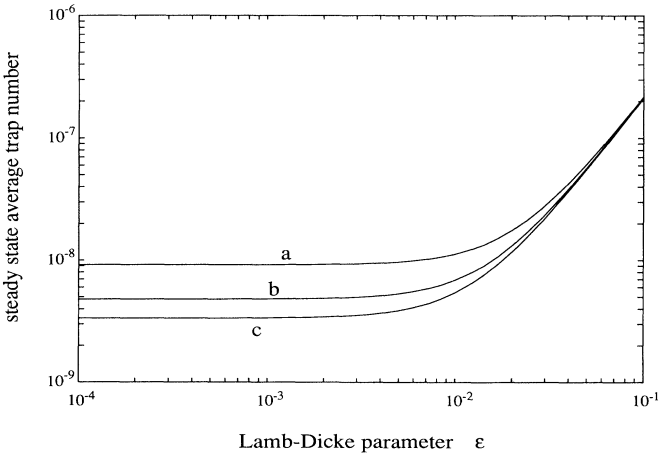

FIG. 7. The steady-state average trap number as a function of the Lamb-Dicke parameter ϵ for various values of the scaled spontaneous emission rate. The parameters used are $N=5$ and $\nu'=100$, with $\Gamma'=0.02,0.01,0.001$, labeled (a)–(c), respectively.

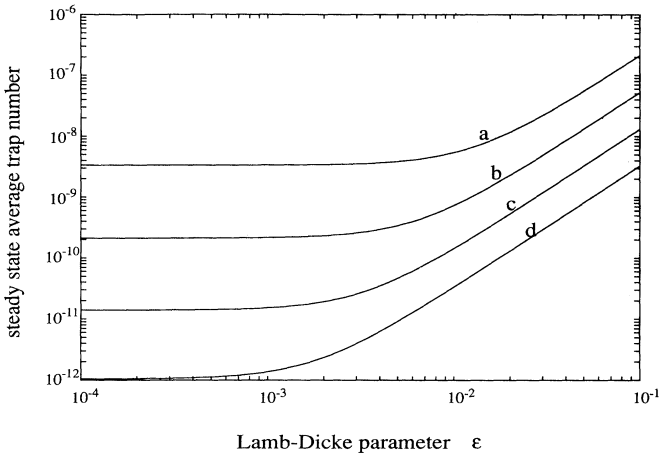

FIG. 8. The steady-state average trap number as a function of the Lamb-Dicke parameter ϵ for various values of the scaled trap frequency. The parameters used are $N=5$ and $\Gamma'=0.001$, with $\nu'=100,200,400,800$, labeled (a)–(d), respectively.

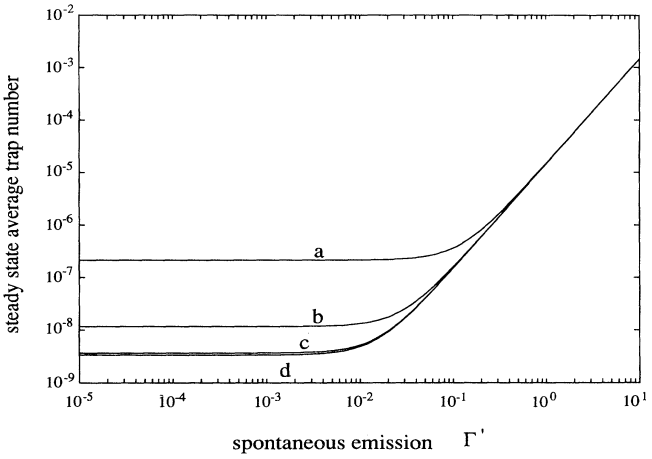

FIG. 9. The steady-state average trap number as a function of the spontaneous emission for various values of the Lamb-Dicke parameter ϵ. The parameters used are $N=5$ and $\nu'=100$, with $\epsilon=0.1,0.01,0.001,0.0001$, labeled (a)–(d), respectively.

between $|g,n+1\rangle$ and $|e,n\rangle$ increases in strength for higher ϵ.

In the sideband cooling experiment of Wineland and co-workers [20] a theoretical value for the steady-state average trap number of $\langle n\rangle\sim10^{-6}$ is obtained. This value is based on the work in [3] and includes the effect of the laser linewidth and micromotion, but it does assume the LDP regime. We have already seen, however, that the single mercury ion system is [20] is in the SSB regime. With experimental values of the order of $\Gamma'\sim2.5\times10^{-5}$ and $\nu'\sim7.5$, the system is in the parameter regime where saturation of the average trap number occurs. The steady-state trap number can, therefore, be described by Eq. (39) and has an order-of-magnitude value of $\langle n\rangle_c\sim10^{-5}$. It should be noted that this cannot be directly compared with the theoretical value quoted in [20] as we have not included the linewidth of the driving field or the micromotion.

V. TIME EVOLUTION

The time evolution of the ion in the trap is governed by the cooling rate γ_c. In the LDP regime the cooling rate is given by

$$\gamma_c=\frac{\epsilon^c}{\Gamma'} \tag{40}$$

to zeroth order in Γ'/ν' for the case where incoherent effects are dominant, $\Gamma'>P(\Delta')$ [7,8]. It might seem more reasonable to expect γ_c to be directly proportional to Γ', but the cooling is essentially due to the $|g,n\rangle\rightarrow|e,n-1\rangle\rightarrow|g,n-1\rangle$ process and the strength of the coherent transition $|g,n\rangle\leftrightarrow|e,n-1\rangle$ goes as $1/\Gamma'$.

We calculate the time evolution of the system in the SSB regime by solving Eq. (23) where the correction terms are evaluated to order $1/\nu'^2$:

$$\dot\rho_{ee}(n,n)=-\Gamma'_{nn}\rho_{ee}(n,n)+\frac{i}{2}[\tilde\rho_{eg}(n,n+1)u^*_{n+1,n}-u_{n,n+1}\tilde\rho_{ge}(n+1,n)]$$
$$+\frac{\Gamma'/4}{\nu'^2+\Gamma'^2/4}[\rho_{gg}(n,n)-\rho_{ee}(n,n)]\ ,$$
$$\dot\rho_{gg}(n,n)=\frac{i}{2}[\tilde\rho_{ge}(n,n-1)u_{n-1,n}-u^*_{n,n-1}\tilde\rho_{eg}(n-1,n)]+\frac{\Gamma'/4}{\nu'^2+\Gamma'^2/4}[\rho_{ee}(n,n)-\rho_{gg}(n,n)]+Q(n,n)\ , \tag{41}$$
$$\dot{\tilde\rho}_{eg}(n,n+1)=-\tfrac{1}{2}\Gamma'\tilde\rho_{eg}(n,n+1)+\frac{i}{2}[\rho_{ee}(n,n)-\rho_{gg}(n+1,n+1)]u_{n,n+1}+C^{(1)}(n)\tilde\rho_{eg}(n,n+1)$$
$$+\sum_{k\ (\neq n)}C^{(2)}(n,k)\tilde\rho_{ge}(k+1,k)+\sum_k C^{(3)}(n,k)\rho_{ee}(k,k)\ ,$$

and $\tilde{\rho}_{ge}(n+1,n)=[\tilde{\rho}_{eg}(n,n+1)]^*$, where

$$C^{(1)}(n)=-\tfrac{1}{4}\sum_{m\,(\neq n)}\frac{|u_{m,n+1}|^2}{i\nu'(n-m)+\Gamma'_{nm}} -\tfrac{1}{4}\sum_{m\,(\neq n+1)}\frac{|u_{m,n}|^2}{i\nu'(m-n-1)}-\frac{1}{i\nu'}\frac{\Gamma'/4}{-i\nu'+\Gamma'_{nn}}\ ,$$

$$C^{(2)}(n,k)=-\frac{\Gamma'_{nk}}{4}\frac{u_{n,k+1}u_{n+1,k}}{[i\nu'(n-k)+\Gamma'_{nk}]i\nu'(n-k)}\ , \tag{42}$$

$$C^{(3)}(n,k)=\frac{i}{2}\Gamma\sum_{m\,(\neq n+1)}\frac{u_{nm}}{i\nu'(n-m+1)}\lambda_{kk}^{(n+1)(m)}\ . \tag{43}$$

The spontaneous emission rate has been modified for a truncated set of equations as in Eq. (35). The recoil term must also be expanded and takes the form

$$Q(n,n)=\Gamma'\sum_k[\,\lambda_{kk}^{(n)(n)}+C^q(n,k)\tilde{\rho}_{eg}(k,k+1) +C^q(n,k)^*\tilde{\rho}_{ge}(k+1,k)]\ , \tag{44}$$

where

$$C^q(n,k)=\frac{i}{2}\Gamma'\sum_{k'\,(\neq k)}\lambda_{kk'}^{(n)(n)}\frac{u_{k+1,k'}}{i\nu'(k-k')+\Gamma'_{nn}}\ . \tag{45}$$

The time behavior of the average trap quantum number $\langle n\rangle$ for different values of the scaled spontaneous emission rate is shown in Fig. 10. The results are obtained by integrating out Eqs. (41) using a Runge-Kutta procedure. The ion is initially in its electronic ground state with its external motion in a thermal state with average trap number $\langle n\rangle_{\rm th}$. When incoherent processes are dominant the cooling rate is inversely proportional to the spontaneous emission rate. When coherent processes are dominant the cooling rate is directly proportional to Γ'. Figure 11 shows the time evolution of $\langle n\rangle$ for various values of the Lamb-Dicke parameter ϵ. In the Lamb-Dicke limit the rate of cooling is directly proportional to ϵ.

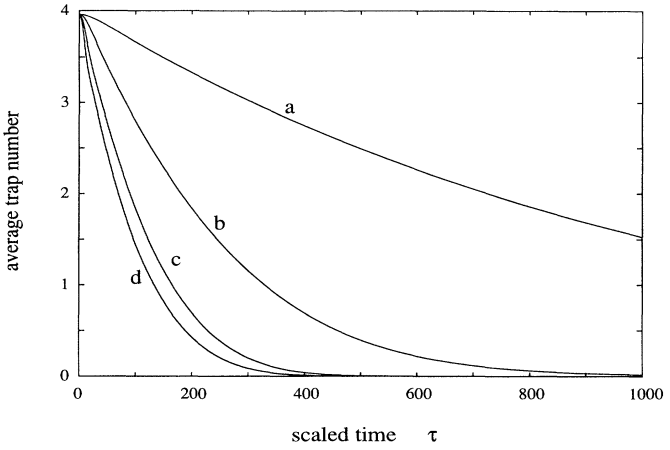

FIG. 11. Time evolution of the average trap number for various values of the Lamb-Dicke parameter. The ion is initially in its ground electronic state and in a thermal state in the trap with $\langle n\rangle_{\rm th}=3.96$. The parameters used are $N=15$, $\Gamma'=0.1$, and $\nu'=100$, with $\epsilon=0.01,0.025,0.05,0.075$, labeled (a)–(d), respectively.

Coherent processes dominate over incoherent when $\Gamma'<\epsilon$, and give rise to oscillations in $\langle n\rangle$, which can be seen in Fig. 10 for $\Gamma'=0.01$. These coherent effects have the same origin as the quantum collapses and revivals in the atomic inversion shown to occur in the trapped ion system [19]. For such behavior to occur the driving field must be tuned for maximum cooling $\Delta'=\nu'$ and also $\nu'\gg 1$ to ensure that oscillation between $|g,n\rangle$ and $|e,n-1\rangle$ is the dominant coherent process. The spontaneous emission rate must also be such that the collapses

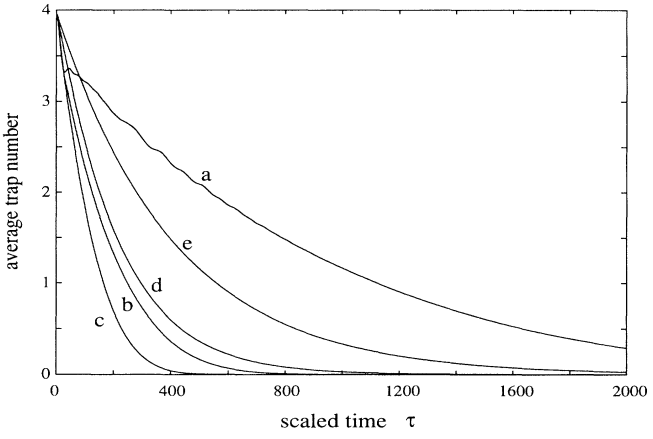

FIG. 10. Time evolution of the average trap number for various values of the spontaneous emission. The ion is initially in its ground electronic state and in a thermal state in the trap with $\langle n\rangle_{\rm th}=3.96$. The parameters used are $N=15$, $\epsilon=0.05$, and $\nu'=1000$, with $\Gamma'=0.01,0.05,0.1,0.5,1$, labeled (a)–(e), respectively.

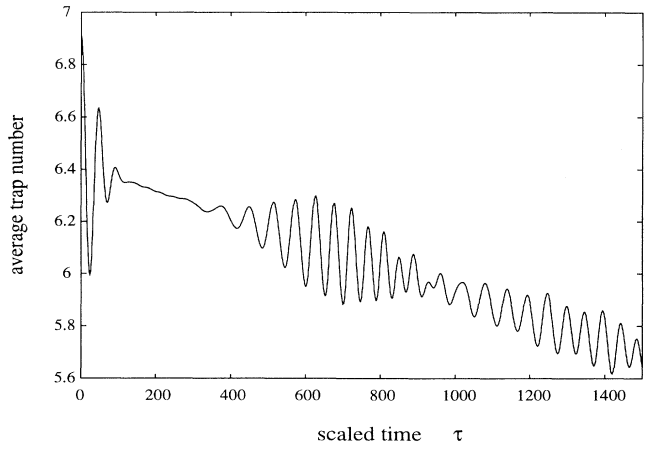

FIG. 12. Time evolution of the average trap number showing quantum collapses and revivals. The ion is initially in its ground electronic state and in a coherent state in the trap with $\langle n\rangle_{\rm coh}=6.9$. The parameters used are $N=15$, $\Gamma'=0.001$, $\nu'=1000$, and $\epsilon=0.05$.

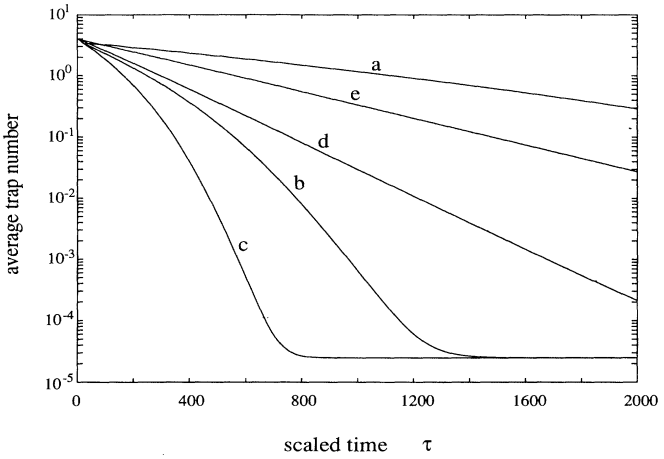

FIG. 13. Time evolution of the average trap number for various values of the spontaneous emission. Parameters are as for Fig. 9.

and revivals are not damped out. Γ' must be chosen, therefore, to satisfy

$$\frac{1}{\Gamma'} < \tau_r \ , \tag{46}$$

where τ_r is the revival time for the oscillations [22,19]. Finally the ion must be prepared in a coherent state in the trap. If these conditions hold the effective Rabi frequency corresponding to oscillation between the states $|g,n\rangle$ and $|e,n-1\rangle$ is a function of the trap quantum number n. The time evolution of the atomic inversion shows collapses and revivals due to dephasing and rephasing between these Rabi oscillations. This behavior can also occur for the average trap quantum number as can be seen in Fig. 12.

There are other effects to be seen in the time behavior due to strong coherent oscillations in the system. The rate of cooling is determined by the real part of the eigenvalues of the system, in particular by the negative real eigenvalue whose absolute value is the smallest. For dominant coherent processes such eigenvalues are of order Γ'. As the most important coherent oscillation is between $|g,n\rangle$ and $|e,n-1\rangle$, some of the imaginary parts of the eigenvalues will be of order $|u_{\bar{n},1+\bar{n}}| \sim \epsilon$. If $\epsilon \geq \Gamma'$ the coherent oscillation may inhibit the decay of the average trap quantum number $\langle n \rangle$. This behavior can be seen in Fig. 13, where Fig. 10 is replotted except for the scale for $\langle n \rangle$ now being logarithmic. The rate of decay is smaller than that expected from the smallest real part of the system eigenvalues, but does accelerate as the transients are damped out. For $\Gamma' > \epsilon$ the more usual linear plot is obtained.

VI. QUANTUM JUMPS

Recently a Monte Carlo simulation of the master equation for a trapped ion has been carried out using atomic wave functions [15]. A large number of simulations were averaged over to give the ensemble time evolution for the system. In this section we look at a single quantum trajectory and carry out a stochastic simulation of the motion of the ion in the trap. We wish to know whether information can be obtained on the jumps made by the ion between different trap states.

For a single ion in a trap, information is carried by the fluorescent photons. The energies of these spontaneously emitted photons will be given by $\omega_{ge} \pm m\nu$ for $m = 0,1,2,\ldots$. If the system is in the Lamb-Dicke limit the majority of fluorescent photons will have $m = 0$ or 1, and in the simulation it will be assumed that these are the only energies occurring. It might be hoped that the measured energy of any particular fluorescent photon would give information on which trap states the ion has jumped between.

There are, however, two difficulties. The first is, that the measurement process does not collapse the wave function into any particular trap state, but rather the ion remains in a coherent superposition of the trap states. It is not possible to say, therefore, between which trap states the ion has jumped. This would not be a difficulty for an anharmonic trap where, in principle, the energy of the fluorescent photon would give information on which trap states the ion jumped between. The second difficulty is that there will be a number of possible coherent processes occurring. An ion in the state $|g,n\rangle$ may be coherently driven into the state $|e,n\rangle$, $|e,n-1\rangle$, or some other excited state. For example, consider the case where the $|g,n\rangle$ state is equally likely to be coherently driven into the state $|e,n\rangle$ or $|e,n-1\rangle$. If a fluorescent photon of energy ω_{ge} is observed it is not possible to say with high probability whether the trap state has changed by zero or one quantum of energy. In general if a fluorescent photon is observed it is impossible to correlate this with a change in the trap state.

However, if the SSB regime is considered, the dominant coherent process is between the states $|g,n\rangle$ and $|e,n-1\rangle$ and there will be a high correlation between fluorescent photons of energy $\omega_{ge}+m\nu$ and changes in the trap state given by $\Delta n = -(m+1)$ (where m is any integer). Likewise in the LDP regime the dominant coherent process is between $|g,n\rangle$ and $|e,n\rangle$. There is, therefore, a high correlation between fluorescent photons of energy $\omega_{ge}+m\nu$ and changes in the trap state given by $\Delta n = -m$.

The simulation will be carried out using the Monte Carlo wave-function approach of [16,17]. As a first step a wave function for the system at time t is written in terms of a set of truncated eigenstates

$$|\psi(t)\rangle = \sum_{n=0}^{N} [g_n(t)|g,n\rangle + e_n(t)|e,n\rangle] \otimes |0\rangle \ , \tag{47}$$

where g_n and e_n are the probability amplitudes for the atom to be in its ground and excited states, respectively, and in the nth trap state. The ground state of the quantized electromagnetic field is represented by the $|0\rangle$, that is, there are no fluorescence photons.

We allow the system to evolve a time dt where $dt \ll \Gamma^{-1}, \Omega_c^{-1}, \Delta_c^{-1}$, and Ω_c and Δ_c are characteristic system Rabi and detuning frequencies. These conditions

ensure that at most one spontaneous photon is emitted between t and $t+dt$. At time $t+dt$ the wave function can be decomposed over the zero- and one-photon manifolds:

$$|\psi(t+dt)\rangle = |\psi^{(0)}(t+dt)\rangle + |\psi^{(1)}(t+dt)\rangle ,$$
$$|\psi^{0}(t+dt)\rangle = \sum_{n=0}^{N} [g_n^{(0)}(t+dt)|g,n\rangle + e_n^{(0)}(t+dt)|e,n\rangle]\otimes|0\rangle , \quad (48)$$
$$|\psi^{(1)}(t+dt)\rangle = \sum_{n=0}^{N} g_n^{(1)}(t+dt)|g,n\rangle \otimes \sum_{\mathbf{k},\lambda} \beta_{\mathbf{k},\lambda}|\mathbf{k},\lambda\rangle ,$$

where $\mathbf{k}$ and λ denote the wave vector and the polarization of the spontaneously emitted photon. It should be mentioned that the sum over the ground states in the expression for $|\psi^{(1)}(t+dt)\rangle$ is due to the fact that the atom can theoretically decay into any trap state. Also there is no contribution from $|e,n\rangle$ to $|\psi^{(1)}\rangle$, because the condition $\Omega dt \ll 1$ ensures that any reexcitation after a decay during dt can be neglected.

The probability of spontaneous emission in the time dt is given by the square of the norm of $|\psi^{(1)}\rangle$ and can be written

$$dp = \Gamma S(t) dt , \quad (49)$$

where $S(t)=\sum_{n=0}^{N}|e_n(t)|^2$ is the probability that the atom will be found in its excited state.

The probability amplitudes $g_n^{(0)}(t+dt)$ and $e_n^{(0)}(t+dt)$ can be obtained by acting on $|\psi(t)\rangle$ with a non-Hermitian Hamiltonian given by Eq. (5) but which includes a spontaneous emission term describing departure rates from the zero-photon manifold. The equations of motion are, for $m=0,\ldots,N$,

$$\dot{g}_m = -i\omega_m^g g_m - \frac{i}{2}\Omega \sum_{n=0}^{N} u_{m,n}^{*} e_n ,$$
$$\dot{e}_m = -i\left[\omega_m^e - i\frac{\Gamma}{2}\right] e_m - \frac{i}{2}\Omega \sum_{n=0}^{N} u_{m,n} g_n . \quad (50)$$

The free oscillation frequencies are $\omega_m^{e,g}=(m+\frac{1}{2})\nu \pm \frac{1}{2}\Delta$, where the plus (minus) corresponds to the excited (ground) state.

We assume that all spontaneously emitted photons are detected by a perfect counter. Depending on the result 0 or 1 for the number of photons detected, the state $|\psi(t+dt)\rangle$ is projected onto $|\psi^{(0)}(t+dt)\rangle$ or $|\psi^{(1)}(t+dt)\rangle$ and the result is normalized. For some pseudorandom number x, uniformly distributed between 0 and 1, if $x > dp$,

$$|\psi(t+dt)\rangle = \mu \sum_{n=0}^{N} [g_n^{(0)}(t+dt)|g,n\rangle + e_n^{(0)}(t+dt)|e,n\rangle]\otimes|0\rangle , \quad (51a)$$

if $x < dp$,

$$|\psi(t+dt)\rangle = \sum_{n=0}^{N} g_n^{(1)}(t+dt)|g,n\rangle \otimes |0\rangle , \quad (51b)$$

with $\mu=(1-dp)^{-1/2}$. We assume that the detected photon has been destroyed and plays no role in the subsequent evolution of the system.

If a spontaneous emission occurs in the interval dt then the wave function after the spontaneous emission is given by

$$\sigma^{-} e^{ik_{ge}\hat{\mathbf{k}}\cdot\mathbf{x}} |\psi(t+dt)\rangle , \quad (52)$$

where $\mathbf{k}=k_{eg}\hat{\mathbf{k}}$ is the wave vector of the spontaneously emitted radiation. The probability amplitude that the atom will be found in the state $|g,n'\rangle$ after the spontaneous emission is given by

$$g_{n'}^{(1)}(t+dt) = \langle g,n'|\sigma^{-} e^{i\tilde{\epsilon}(a+a^{\dagger})}|\psi(t+dt)\rangle = \sum_{n} u_{n,n'}(\tilde{\epsilon}) e_n(t) , \quad (53)$$

where $\tilde{\epsilon}=\epsilon\cos\theta$ and θ is a random number chosen from between 0 and 2π.

The spontaneous emission can occur between any two trap states, and we shall need to be able to calculate the relative probabilities of spontaneous emission between the trap states n and n'. The transition amplitude for the system to be taken from $|e,n\rangle$ to $|g,n'\rangle$ by spontaneous emission is $T(n\rightarrow n')=\langle g,n'|\sigma^{-} e^{ik_{ge}\hat{\mathbf{k}}\cdot\mathbf{x}}|e,n\rangle = u_{n,n'}(\tilde{\epsilon})$. To obtain the transition probabilities for all possible spontaneous emission events which change the trap state by m we sum over the upper state probabilities:

$$R(\Delta m) = \sum_{n} |T(n\rightarrow n+\Delta m)|^2 |e_n|^2 . \quad (54)$$

In the Lamb-Dicke regime only $\Delta m = 0, \pm 1$ are of interest and the three probabilities in Eq. (54) can now be normalized to unity and a pseudorandom number x can be used to decide which of the fluorescent photon energies, ω_{ge}, $\omega_{ge}+\nu$, or $\omega_{ge}-\nu$, is most likely to occur.

A single stochastic simulation is shown in Fig. 14. The

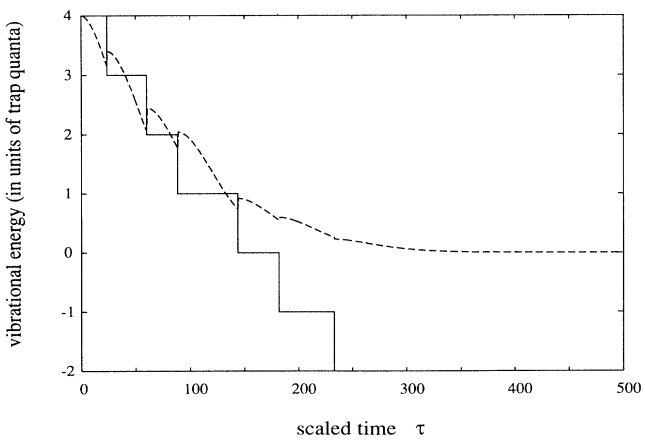

FIG. 14. A single simulation of an ion in a trap showing the change in the vibrational energy in units of $\hbar\nu$. The dotted line gives the ensemble average for the vibrational energy. The parameters used are $\nu'=\Delta'=1000$, $\Gamma'=0.1$, $\epsilon=0.05$, $N=15$, and $\bar{n}_{\mathrm{coh}}=4$.

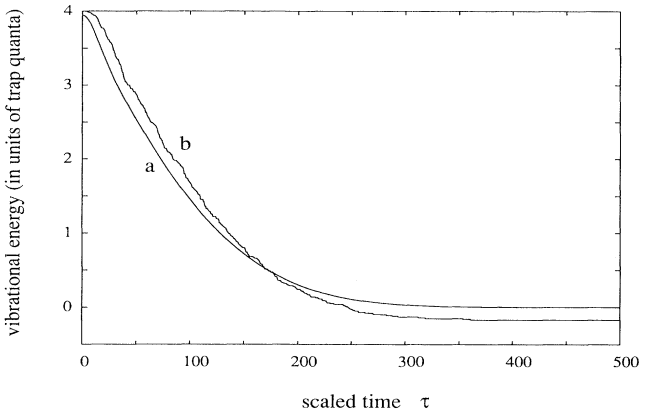

FIG. 15. The change in trap state in units of $\hbar\nu$ for (a) an ensemble average as calculated for Fig. 13, and (b) for an average over 100 stochastic simulations. The parameters are the same as those used in Fig. 13.

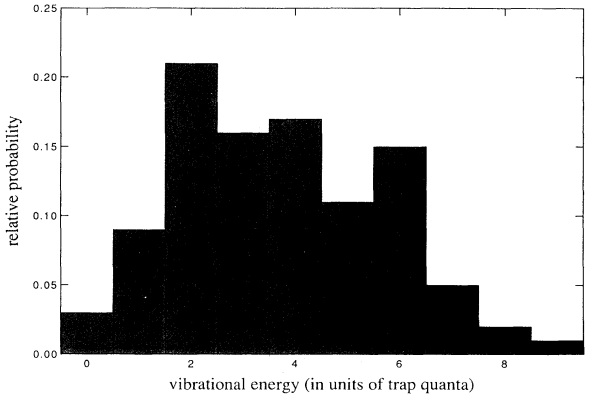

FIG. 16. The relative probability of extracting $n\hbar\nu$ vibrational energy from an ion in a trap. The parameters used are $\nu'=\Delta'=1000$, $\Gamma'=0.1$, $\epsilon=0.05$, $N=15$, $N_E=100$, and $\bar{n}_{\rm coh}=4$.

ion starts in a coherent state in the trap with average trap number $\bar{n}_{\rm coh}=4$. Also shown on the graph is the ensemble average of the trap number obtained by calculating $|g_n(t)|^2+|e_n(t)|^2$. This exhibits discontinuous jumps at the times that spontaneous emissions occur. It can be seen that although the ensemble average shows $4\hbar\nu$ energy lost from the trap, the stochastic simulation shows $6\hbar\nu$ energy lost from the trap. Certainly in this single case there is not a good correlation between the number of jumps inferred from the spontaneously emitted photons and the average number of trap quanta lost in the cooling process. The reason for this comes from the randomizing influence of the spontaneous emission in its action on the ion wave function [Eq. (52)].

In the case that the characteristic Rabi frequency Ω_c is of the same order of magnitude or larger than the spontaneous emission, the ion may undergo several Rabi cycles before spontaneous emission occurs. In such a case the probability distribution over the trap states rapidly loses its Poissonian character. When spontaneous emission does occur the average trap number for the upper electronic state may be quite different from the average trap number for the upper and lower electronic states together. This can lead to a large increase or decrease in the average trap number. While such events may not conserve energy individually an average over a number of stochastic simulations should give behavior approaching the ensemble average (Fig. 15).

In Fig. 15 the average trap number is calculated by averaging over $N_E=100$ stochastic simulations. For each individual simulation the relative change in the trap state can be calculated. The correlation between a trap with average vibrational energy $\bar{n}$ and observing a change $\Delta n\hbar\nu$ in the trap energy can be calculated from the relative probabilities of seeing a certain relative change in the trap state. For the $N_E=100$ simulations carried out leading to Fig. 15 the relative probabilities are shown in Fig. 16. For an ion prepared in a coherent state with $\bar{n}_{\rm coh}=4$ the probability of observing a change of $4\hbar\nu$ in the trap energy is only 0.25. It should be stressed that the relative probabilities given in Fig. 16 do not constitute ensemble behavior as the sample size is only $N_E=100$.

VII. CONCLUSION

The analytic results obtained for sideband cooling of an ion or atom in a harmonic trap are valid only in the so-called Lamb-Dicke perturbation regime, where the Lamb-Dicke parameter ϵ is taken to be sufficiently small compared with unity such that the strongest coherent oscillation occurs between the states with the same trap quantum number. This paper is a discussion of the so-called strong-sideband regime, where the parameter $(\Gamma'/2\nu'\epsilon)^2$ is much smaller than unity, such that the dominant coherent oscillation occurs between the states $|g,n\rangle$ and $|e,n-1\rangle$.

In the LDP regime the equations of motion for the master equation decouple to zeroth order in the Lamb-Dicke parameter, which enables analytic solutions to be found. In the SSB regime all the states of the system are coupled together to lowest order in $1/\nu'$, which makes it impossible to find analytic solutions to the equations of motion. A perturbation expansion in the small parameters $1/\nu'$, Γ'/ν', and ϵ/ν' is developed which reduces the dimension of the problem from $4(N+1)^2$ to $4(N+1)$, where N is the trap number at which the equations of motion are truncated.

This perturbation expansion leads to a semiquantitative discussion of saturation effects for the final cooling energy. It is shown that the steady-state average trap number saturates for small values of the spontaneous emission rate. It is also shown that for spontaneous emission rates much smaller than the trap frequency the steady-state average trap number $\langle n\rangle$ goes inversely as the fourth power of the trap frequency, rather than as the second power when not in the saturation region. It is also argued that the sideband cooling experiment of Wineland and co-workers [20] is carried out in the SSB regime.

Simulations of the time evolution are also presented.

There are various transient coherent effects present in the system including inhibition of the decay of the average trap number $\langle n \rangle$ and quantum collapses and revivals in $\langle n \rangle$.

In the final section of this paper we have asked whether it is possible to observe the jumps made by an ion between different trap states as the cooling progresses. In particular, is there a high correlation between the vibrational energy lost from the ion and the average vibrational energy in the trap before cooling? We have carried out a simulation in the regime where $\Omega_c \sim \Gamma$, as this minimizes computer time. These simulations show that for a single quantum trajectory the correlation is not high.

ACKNOWLEDGMENTS

We would like to thank Dr. M. J. Collett and Dr. S. M. Tan for helpful discussions. The work was supported by the University of Auckland Research Committee, the New Zealand Vice Chancellors Committee, the N.Z. Lottery Grants Board, and I.B.M New Zealand.

[1] W. Neuhauser, M. Hohenstatt, P. Toschek, and H. Dehmelt, Phys. Rev. Lett. **41**, 233 (1978).
[2] D. J Wineland and W. M. Itano, Phys. Rev. A **20**, 1521 (1979).
[3] D. J. Wineland, W. M. Itano, J. C. Bergquist, and R. G. Hulet, Phys. Rev. A **36**, 2220 (1987).
[4] J. Javanainen and S. Stenholm, Appl. Phys. **21**, 283 (1980).
[5] J. Javanainen and S. Stenholm, Appl. Phys. **24**, 71 (1981).
[6] J. Javanainen and S. Stenholm, Appl. Phys. **24**, 151 (1981).
[7] J. Javanainen, M. Lindberg, and S. Stenholm, J. Opt. Soc. Am. B **1**, 111 (1984).
[8] M. Lindberg and S. Stenholm, J. Phys. B **17**, 3375 (1984).
[9] S. Stenholm, Rev. Mod. Phys. **58**, 699 (1986).
[10] R. J. Cook and H. J. Kimble, Phys. Rev. Lett. **54**, 1023 (1985).
[11] W. Nagourney, J. Sandberg, and H. Dehmelt, Phys. Rev. Lett. **56**, 2797 (1986).
[12] Th. Sauter, W. Neuhauser, R. Blatt, and P. E. Toschek, Phys. Rev. Lett. **57**, 1696 (1986); Th. Sauter, R. Blatt, W. Neuhauser, and P. E. Toschek, Opt. Commun. **60**, 287 (1986).
[13] J. C. Bergquist, R. G. Hulet, W. M. Itano, and D. J. Wineland, Phys. Rev. Lett. **57**, 1699 (1986).
[14] W. M. Itano, J. C. Bergquist, R. G. Hulet, and D. J. Wineland, Phys. Rev. Lett. **59**, 2732 (1986).
[15] R. Dum, P. Zoller, and H. Ritsch, Phys. Rev. A **45**, 4879 (1992).
[16] C. Cohen-Tannoudji, F. Bardou, and A. Aspect, in *Laser Spectroscopy X*, edited by M. Ducloy, E. Giacobino, and G. Camy (World Scientific, Singapore, 1992).
[17] J. Dalibard, Y. Castin, and K. Mølmer, Phys. Rev. Lett. **68**, 580 (1992).
[18] W. H. Louisell, *Quantum Statistical Properties of Radiation* (Wiley, New York, 1973).
[19] C. A. Blockley, D. F. Walls, and H. Risken, Europhys. Lett. **17**, 509 (1992).
[20] F. Diedrich, J. C. Bergquist, W. M. Itano, and D. J. Wineland, Phys. Rev. Lett. **62**, 403 (1989).
[21] J. C. Bergquist, D. J. Wineland, W. M. Itano, H. Hemmati, H.-U. Daniel, and G. Leuchs, Phys. Rev. Lett. **55**, 1567 (1985).
[22] N. B. Narozhany, J. J. Sanchez-Mondragon, and J. H. Eberly, Phys. Rev. A **23**, 236 (1981).